Progress In Electromagnetics Research, PIER 104, 267–282, 2010

AN AUTOMATIC MODEL ORDER REDUCTION OF A UWB ANTENNA SYSTEM

Z. Zhang and Y. H. Lee

School of Electrical and Electronic Engineering
Nanyang Technological University
Singapore

Abstract—This paper proposes an efficient and automatic means of achieving a reduced model of a transfer function for UWB antenna design. According to the formulation of a transfer function, we have derived two factors, which are critical in determining the radiation pattern and input impedance respectively. Their special formula allow us to establish a reduced model automatically using the Model Order Reduction (MOR) techniques of a second order system. The process is free of any human factors and suitable to any antenna systems, thus enabling a direct and efficient interface with the optimization process in the design of a UWB antenna system. In addition, the proposed way of establishing a transfer function of the whole antenna system has successfully cascaded the entire system into separate subsystems, thus offering deeper insights in analyzing a UWB antenna system.

1. INTRODUCTION

Ultra wideband (UWB) antenna design has become one of the hottest topics in the field of antenna design. However, to design a functionally desirable antenna for UWB use is a really tough task. The primary challenge is how to characterize the antenna system effectively. The concept of transfer function [1–3] leads to a proper understanding of a UWB antenna system. However, to determine the transfer function over an ultra-wide band entails expensive computational cost. In order to address this difficulty, solutions have been widely discussed. Amongst them, the way of reducing the discrete responses into an analytical model [4–7] attracts growing attentions. This approach has successfully circumvented the requirement of obtaining the responses to

Corresponding author: Z. Zhang (zhangzhan@pmail.ntu.edu.sg).

sufficient resolution, by instead constructing a physical-based reduced model on the basis of much fewer samples. Since only some samples at selected frequencies are needed to be computed directly, the efficiency of characterization has been highly enhanced. In addition, the other benefits, such as unifying the spectral and temporal representations and favoring an analytic operation with the rest of the system, make this approach even more appealing.

In fact, some efforts has been already made in the derivation of a reduced model for the transfer function and some successful works has been reported in the literatures. However, the majority of them are based on the method of Model Based Parameter Estimation (MBPE) [4–7]. The core idea is to assume a generic model first and then to estimate the parameters via extracting the useful information from the samples. Since the whole process is free of any specific knowledge, MBPE is applicable to virtually all of electromagnetic problems, thus earning overwhelming popularity. Although MBPE opens the possibility of fulfilling a reduced model of a transfer function, it shows some limitations especially as applying it to the optimized design of a UWB antenna. As a sample-based method, MBPE is highly sensitive to the choices of samples. Although the good result can be expected, its success is mainly depended on the human efforts in carefully tuning the number and locations of the samples. As a result, it is far from an automatic process, thus failing to provide a direct and automatic interface with a well-programmed optimization code, such as Genetic Algorithm (GA) and Particle Swarm Optimization (PSO). Despite the extensive efforts made to reduce the uncertainties arising in the sample selection [9, 10], a self-generated reduced model without any human factors can not be achieved using MBPE.

Since optimization has become an indispensable part in nowadays antenna design, the desire of working with a human-free optimization code raises a new challenge and has motivated our work to seek a reduced model of the transfer function automatically. Turning a shift from MBPE that is heavily depended on the samples, this paper proposed a new way that is based on the physical description of the transfer function. At the first step, we take a careful investigation on the formulation of a transfer function and then derive two complex factors that determines the characteristics of the input admittance and the radiation pattern of the antenna system respectively. Based on them, a transfer function can be fully established. It is interesting to find that the forms of both factors are consistent with the classic descriptor of a dynamic system. In addition, impedance matrix, $\mathbf{Z}(s)$, constitutes the transformation matrix of the both, which implies that they would have the identical poles. Proper segmentation enables $\mathbf{Z}(s)$

exhibited in each segment to be approximated by a quadratic function. Thus, a second order system is established within each segment. The corresponding dominant poles and residues are simultaneously identified by Q-arnoldi method [11], an efficient MOR method for a second-order system. Gathering them from each segment results in a reduced model ultimately. This process is free of any human factors. Additionally, establishing the transfer function upon two separate models offers more flexibility in dealing with various feeding systems or propagation channels.

This paper is organized as follows. Section 2 gives a basic formulation of problem. Section 3 describes the process of MOR. Numerical results and conclusions are given in Sections 4 and 5.

2. PROBLEM FORMULATION

We can take a full view of a UWB communication architecture from three ports represented by source signal $V_s(s)$ at the feeding, radiated field $E_{rad}(s)$ at a far point and output signal $V_{out}(s)$ at the loading. By properly assigning the input and the output, the resulting transfer function serves to portray the filtering property of the intermediate system.

$$H_{TA}(s) = \frac{E_{rad}(s)}{V_s(s)} \tag{1}$$

$$H_{RA}(s) = \frac{V_{out}(s)}{E_{rad}(s)} \tag{2}$$

$$H(s) = \frac{V_{out}(s)}{V_s(s)} \tag{3}$$

where $s = j2\pi f$, f is the frequency. For the present purpose, the definitions are assumed only frequency-dependent, while ignoring the other factors such as the polarization and angular dependence. According to the above definitions, $H_{TA}(s)$, namely transmitting antenna transfer function takes into account the transmitting antenna (Tx) and the channel jointly, whereas the receiving antenna transfer function, $H_{RA}(s)$ only consider the transfer properties of the receiving antenna (Rx). As integrating them together, $H(s)$ is taken as the overall response of the whole system. This paper will concentrate on the modeling of $H_{TA}(s)$ and then exploit the reciprocity to derive $H_{RA}(s)$ of the same antenna. Based on $H_{TA}(s)$ and $H_{RA}(s)$ and given the both polarization of Tx and Rx, $H(s)$ can be derived accordingly. The following discussions are developed by the moment of method relying on Rao-Wilton-Glisson (RWG) basis function [12, 13].

However, the similar analysis can be arrived depending on the other basis function for solving electrical field integral equation (EFIE). For convenience, we start with some basic concepts of RWG edge elements. Suppose the antenna surface is divided into separate triangles, each pair of triangles sharing an edge in common constitutes a basic element and is distinguished by a plus sign T^+ and a minus sign T^- such that the reference current is always from T^+ to T^-. A basis function is assigned to each edge as following:

$$\mathbf{f}(\mathbf{r}) = \begin{cases} l/2A^+\rho^+(\mathbf{r}) & \mathbf{r} \text{ in } T^+ \\ l/2A^-\rho^-(\mathbf{r}) & \mathbf{r} \text{ in } T^- \\ 0 & \text{otherwise} \end{cases} \tag{4}$$

here l is the length of the edge, $A^\pm$ are the area of $T^\pm$. Vector ρ^+ connects the free vertex of T^+ to the observation point $\mathbf{r}$, whereas ρ^- connects the observation point $\mathbf{r}$ to the free vertex of T^-. The above way of defining a basis function allows us to consider each edge element as a small but finite dipole of length $|\mathbf{r}^{c-} - \mathbf{r}^{c+}|$ and with a unit current density. Index c denotes the center of $T^\pm$.

In a MoM solver, $H_{TA}(s)$ can be formulated as

$$H_{TA}(s) = \frac{E_{rad}(s)}{V_{in}(s)} \frac{V_{in}(s)}{V_s(s)} = \frac{E_{rad}(s)}{V_{in}(s)} \frac{Z_A(s)}{Z_A(s) + Z_s(s)} \tag{5}$$

The former part describes the efficiency of radiation where $V_{in}(s)$ is the incident voltage across the antenna, while the latter part corresponds to the impedance matching where $Z_A(s)$ and $Z_s(s)$ are the impedance of the transmitting antenna and the source respectively.

In a MoM, the first step is to solve surface current density $\mathbf{I}(s)$.

$$\mathbf{I}(s) = \mathbf{Z}(s)^{-1}\mathbf{b}\, V_{in}(s) \tag{6}$$

where $\mathbf{Z}(s) \in \mathbb{C}^{n\times n}$ is an impedance matrix and $\mathbf{b}$ denotes an excitation vector. The form of $\mathbf{b}$ depends on the feeding model. In the simplest case a delta-function generator is adopted, $\mathbf{b}$ is supposed to be all zeros, except for the feeding edge m where $\mathbf{b}(m) = l_m$ (l_m is the length of edge m). An alternative model is a base-driven monopole whose feeding model is at a junction of two edge elements, say n_1 and n_2. Similarly, $\mathbf{b}$ is supposed to be all zeros, except that $\mathbf{b}(n_i) = l_{n_i}$, $i = (1, 2)$ (where l_{n_i} is the length of edge n_i). Despite the different forms of feeding model, the antenna impedance $Z_A(s)$ can be generalized to

$$Z_A(s) = \frac{1}{\mathbf{b}^T\mathbf{Z}(s)^{-1}\mathbf{b}} \tag{7}$$

If adopting the delta generator, $Z_A(s)$ equals to $V_{in}(s)/I_m l_m$. Otherwise, $Z_A(s)$ is transformed to $V_{in}(s)/(I_{n1}l_{n1} + I_{n2}l_{n2})$ for the

case of a monopole model. The generalized form of $Z_A(s)$ is validated since it offers a total agreement with the results presented in [13].

Once surface current density $\mathbf{I}(s)$ has been solved, $E_{rad}(s)$ in the far field can be approximated by

$$E_{rad}(s) = \frac{s\eta}{4\pi c}\ \frac{e^{\frac{-sR}{c}}}{R}\ \mathbf{c}^T\ \mathbf{I}(s) \tag{8}$$

where $\mathbf{c}$ is a vector describing the contribution of each edge element to the total field. If each edge element can be treated as an infinitesimal dipole $(r_m^{c-} - r_m^{c+})$ and with an effective current l_m, the mth element of $\mathbf{c}$ corresponds to $(\mathbf{r}\cdot\mathbf{m})\vec{r}/|\mathbf{r}|$ where $\mathbf{r}$ is the location of observation point and $\mathbf{m} = (r_m^{c-} - r_m^{c+})l_m$.

According to (6), (7) and (8), we develop $H_{TA}(s)$ into

$$\begin{aligned} H_{TA}(s) &= \frac{E_{rad}(s)}{V_{in}(s)}\frac{Z_A(s)}{Z_A(s)+Z_s(s)} \\ &= \frac{s\eta}{c}\frac{e^{\frac{-sR}{c}}}{4\pi R}\mathbf{c}^T\mathbf{Z}(s)^{-1}\mathbf{b}\frac{1}{1+Z_s(s)\mathbf{b}^T\mathbf{Z}(s)^{-1}\mathbf{b}} = \frac{s\eta}{c}\frac{e^{\frac{-sR}{c}}}{4\pi R}\frac{Q_1}{1+Z_s(s)Q_2} \end{aligned} \tag{9}$$

Factoring the linear term $\frac{s\eta}{c}$ and propagation term $\frac{e^{\frac{-sR}{c}}}{4\pi R}$ out, we extract two models: $Q_1(=\mathbf{c}^T\mathbf{Z}(s)^{-1}\mathbf{b})$ and $Q_2(=\mathbf{b}^T\mathbf{Z}(s)^{-1}\mathbf{b})$. Q_1 relates radiation pattern and Q_2 represents the input admittance. As shown in (9), they constitute the critical parts of $H_{TA}(s)$ and the following discussion would further verify that they also act as determining factors in $H_{RA}(s)$.

As well known, the effective length of the antenna, h_{eff}, keeps identical in the mode of the transmission and reception. In terms of Q_1 and Q_2, h_{eff} takes on a new form through the derivation of (10)

$$\frac{s\eta}{c}\frac{e^{\frac{-s}{c}R}}{4\pi R}h_{\text{eff}} = \frac{E_{rad}(s)}{I_{in}(s)} = \frac{E_{rad}(s)}{V_{in}(s)}\frac{V_{in}(s)}{I_{in}(s)} = \frac{s\eta}{c}\frac{e^{\frac{-s}{c}R}}{4\pi R}\frac{Q_1}{Q_2} \Rightarrow h_{\text{eff}} = \frac{Q_1}{Q_2} \tag{10}$$

By exploiting the reciprocity of h_{eff}, $H_{RA}(s)$ of the same antenna can be simply derived from (11), suppose it is loaded by Z_L [14].

$$H_{RA}(s) = h_{\text{eff}}\left(\frac{Z_L}{Z_s(s)+Z_L}\right) = \frac{Q_1}{Q_2}\left(\frac{Z_LQ_1}{1+Z_LQ_2}\right) \tag{11}$$

It should be noted that the same formulation of $H_{RA}(s)$ can be derived by instead solving a receiving problem based on RWG elements [12]. According to (9) and (11), Q_1 and Q_2 determine the complex properties of $H_{TA}(s)$ and $H_{RA}(s)$. Once they are known, the derivation of $H_{TA}(s)$ and $H_{RA}(s)$ becomes trivially simple. Rather than undertaking the model reduction on h_{eff} or directly on the integral transfer function

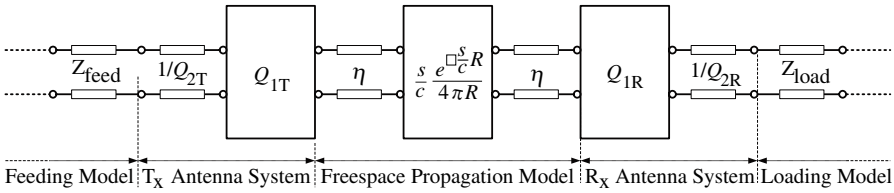

Figure 1. Cascaded system.

by previous work [5, 7, 14], the current study attempts to carry out the modeling on Q_1 and Q_2. One reason is that the formula of Q_1 and Q_2 are both consistent with the generic descriptor of a dynamic system where the techniques of MOR have reached a mature level, thus straightening the possibility of realizing an automatic modeling. Since both models have the identical poles that coincide with the eigenvalues of $\mathbf{Z}(s)$, MOR can proceed on Q_1 and Q_2 simultaneously. Furthermore, the independent analysis of Q_1 and Q_2 lead to a deeper understanding of the entire system which allow us to decompose it into a cascade of subsystems as depicted in Fig. 1. $1/Q_{2T}$ and $1/Q_{2R}$ represent the impedance of Tx and Rx respectively. Their characteristics provide guidelines for design or analysis of the ahead feeding model and the sequent loading model respectively. Similarly, Q_{1T} and Q_{1R} are helpful for investigating the radiation/reception phenomena that taken place on the Tx and Rx respectively. Therefore, the independent modeling of Q_1 and Q_2 offers more details of the antenna system.

3. MODEL REDUCTION OF Q_1 AND Q_2

The following work focus on the modeling of Q_1 and Q_2 which depends on the MOR techniques for a complex electronic system. The core idea is to project a larger system $Q(s)$ into a much smaller one such that the identification of poles (s_i) and residues (R_i) becomes rather simpler. And hence, a reduced model can be established as

$$Q(s) = \sum \frac{R_i}{s - s_i} \tag{12}$$

However,the techniques is highly depended on the complexity order of the system. According to (9), the form of $\mathbf{Z}(s)$ determines the order of both models. Since frequency behavior of $\mathbf{Z}(s)$ can be approximated by a quadratic function [15], it might raise a second-order problem. However, a single quadratic function seems inadequate to depict the complete behavior of $\mathbf{Z}(s)$ over the ultra-wide band. Under such a situation, segmentation of $\mathbf{Z}(s)$ seems necessary. As a

result, the entire system is cascaded into several second-order systems. This requires MOR to be performed within each spectrum separately. Since the dominant behavior of a model is naturally governed by the poles with larger residues and smaller real parts, instead of the full set, computation with special emphasis on those dominant ones leads to increased efficiency. Furthermore, there should be means to compensate the truncated poles out of the investigation band. In sum, the main steps of the method are outlined here:

(i) Segmentation and derivation of $\mathbf{Z}(s)$ of each segment.
(ii) Identification of dominant poles/residues within each spectrum.
(iii) Compensation of the modes out of the spectrum of interest.

3.1. Quadratic Approximation of $\mathbf{Z}(s)$

Using RWG basis functions [12], the impedance matrix is derived by

$$Z_{mn} = l_m[j\omega(A^+_{mn} \cdot \rho^{c+}_m/2 + A^-_{mn} \cdot \rho^{c-}_m/2) + (\Phi^+_{mn} - \Phi^-_{mn})] \quad (13)$$

where the index m and n corresponds to two edge elments; $(\cdot)$ denotes the dot production. A_{mn} and Φ_{mn} represent the magnetic vector potential and the scalar potential as following

$$\begin{aligned} A^{\pm}_{mn} &= \frac{\mu}{4\pi}\left(\frac{l_n}{2A^+_n}\int_{T^+_n}\rho^+_n(r')g^{\pm}_m(r')dS' + \frac{l_n}{2A^-_n}\int_{T^-_n}\rho^-_n(r')g^{\pm}_m(r')dS'\right) \\ \Phi^{\pm}_{mn} &= \frac{1}{4\pi j\omega\epsilon}\left(\frac{l_n}{2A^+_n}\int_{T^+_n} g^{\pm}_m(r')dS' - \frac{l_n}{2A^-_n}\int_{T^-_n} g^{\pm}_m(r')dS'\right) \end{aligned} \quad (14)$$

where $g^{\pm}_m(r') = \frac{e^{-jk|r^{c\pm}_m - r'|}}{|r^{c\pm}_m - r'|}$. From the above expressions, frequency-dependent terms in $\mathbf{Z}(s)$ involves $\omega e^{-jk\triangle r}$ and $e^{-jk\triangle r}/\omega$ where ω is angular frequency, k is the wavenumber and $\triangle r = |r^{c\pm}_m - r'|$. We can further factorize them into $e^{-jk\triangle r}$, ω and $1/\omega$. Among these three factors, $e^{-jk\triangle r}$ has the strongest response to frequency. Therefore, it is a dominant factor of $\mathbf{Z}(s)$. Quadratic function can approximate $e^{-jk\triangle r}$ to certain bandwidth but is subject to a constraint [16]. If the quadratic approximation is made within the band $[f_0 - \triangle f, f_0 + \triangle f]$ that is centered at f_0 and has a symmetrical span of $2\triangle f$, one should make sure that the phase change introduced by $\triangle f$ is strictly less than π in the whole antenna scale [16]. In other words, a necessary condition is that $\triangle k R_{\max} \leq \pi$ where $\triangle k$ is the wavenumber step. To meet such a condition, the maximal frequency step $\triangle f_{\max}$ or the half bandwidth should be limited to $c/(2R_{\max})$ according to (15), where $R_{\max}$ denotes the maximal extent of the antenna, i.e., the maximum of $\triangle r$

$$\triangle k R_{\max} \leq \pi \Rightarrow \triangle f_{\max} \leq c/(2R_{\max}) \quad (15)$$

Although $e^{-jk\triangle r}$ plays a dominant role, the contributions from ω and $1/\omega$ also should be considered. In the next step, we expand them around f_0.

$$\begin{aligned} \omega &= (2\pi f_0)(1 + \triangle f/f_0) \\ 1/\omega &= (1/2\pi f_0)(1 + (-\triangle f/f_0) + \cdots + (-\triangle f/f_0)^n) \end{aligned} \tag{16}$$

Both in terms of $\triangle f/f_0$, the complications introduced by ω and $1/\omega$ challenges the quadratic approximation, especially when $\triangle f/f_0$ turns large. Therefore, to keep $\triangle f/f_0$ sufficiently small is the other necessary condition to justify the quadratic approximation. From our observations, as $\triangle f/f_0 < 1/3$, contributions of high-order terms in (16) becomes negligible, which suggests that the dominant response remains in a quadratic form. Therefore, besides $\triangle f < \triangle f_{\max}$, $\triangle f$ should satisfy the other condition that $\triangle f/f_0 < 1/3$. In order to satisfy the both, the maximum frequency step or the half of the bandwidth should be limited to the lesser between $\triangle f_{\max}$ and $f_0/3$, or simply interpreted as $\min(f_0/3, \triangle f_{\max})$. Therefore, specifying the bandwidth to $2\min(f_0/3, \triangle f_{\max})$ leads to a reliable quadratic function for each segment. To be noted, a segment can be alternatively defined as $[f_s, f_s + 2\min(f_s/2, \triangle f_{\max})]$ or $[f_e - 2\min(f_e/4, \triangle f_{\max}), f_e]$, if the starting point f_s or ending point f_e is known. In fact, the solution to an effective segmentation is not unique. However, good results can be expected simply by following the above guidelines. Here, we recommend one of the most natural ways whereby the first segment is determined by the low end, f_L or the high end, f_H of the whole spectrum, and then segmentation proceeds forwards or backwards until ending up with the other end. Suppose the segments are connected end to end, the other node of a segment can be properly defined by the known one and the process of segmentation can be illustrated by by following recursion, where $f(n)$ and $f(n+1)$ correspond to the beginning and ending node of the nth segment.

$$\begin{aligned} f_{n+1} &= f_n + 2\min(f_n/2, \triangle f_{\max}) \qquad \text{with} \quad f_1 = f_L \\ f_{n+1} &= f_n - 2\min(f_n/4, \triangle f_{\max}) \qquad \text{with} \quad f_1 = f_H \end{aligned} \tag{17}$$

So far, we have successfully divided the entire band into small segments and each one corresponds to a quadratic function of $\mathbf{Z}(f)$: $\mathbf{Z}(f) = \mathbf{M}f^2 + \mathbf{C}f + \mathbf{K}$. The coefficient matrices $\mathbf{M}$, $\mathbf{C}$ and $\mathbf{K}$ can be estimated given $\mathbf{Z}(f)$ at any three frequency points within the segment. Prior to the pole identification, however, $\mathbf{Z}(f)$ should be transformed to the s-plane. If quadratic function of $\mathbf{Z}(f)$ is valid within a segment $[f_s, f_e]$, its counterpart $\mathbf{Z}(s)$ is fully justified along the truncated axis of $[j2\pi f_s, j2\pi f_e]$. Since dominant poles are those with near-zero real part, one can extend $\mathbf{Z}(s)$ to estimate them only if their imaginary part

is restricted to $[2\pi f_s, 2\pi f_e]$. Since the poles/residues come as conjugate pairs, we only need to consider the poles with real frequency. Gathering the dominant poles s_i from each spectrum establishes a model as

$$Q(s) = \sum \frac{R_i}{s - s_i} + \sum \frac{R_i^*}{s - s_i^*} \tag{18}$$

3.2. Dominant Pole Identification Using Q-arnoli

Compared to the mature level of the techniques for the linear system [17], the development of second-order techniques is a relatively new topic, but has raised growing interest, including Second Order Arnoldi [18], Second order dominant pole identification [19] and Quadratic Arnoldi algorithm [11]. In this paper, Quadratic Arnoldi algorithm (Q-arnoldi) are adopted as the numerical method, in terms of its remarkable feature of favoring the convergence to the particular eigenvalues using the strategies of implicit restarting or purging [17]. Known as a memory-efficient and structure-preserving, the core step of Q-arnoldi is to project a large quadratic system into a subspace of much smaller dimension via Krylov recurrence relation [11]. In the reduced subspace, eigentriplets $(s_i, \mathbf{x}_i, \mathbf{y}_i)$ of the original system can be approximated in a much simpler and efficient way, where s_i denotes the eigenvalue, $\mathbf{x}_i$ and $\mathbf{y}_i$ are the left and right eigenvectors. Since the poles of Q_1 and Q_2 are identical, they can be computed simultaneously but their residues have to be computed separately via Q-arnoldi. As to a model $Q(s) = \mathbf{c}^T(\mathbf{M}s^2 + \mathbf{K}s + \mathbf{C})^{-1}\mathbf{b}$, its residues can be estimated by $R_i = (\mathbf{c}^*\mathbf{x}_i)(\mathbf{y}_i^*\mathbf{b})s_i$ provided that $\mathbf{x}_i$ and $\mathbf{y}_i$ are well-scaled so that $-\mathbf{y}_i^*\mathbf{K}\mathbf{x}_i + s_i^2\mathbf{y}_i^*\mathbf{M}\mathbf{x}_i = 1$ [19].

In this paper, Q-arnoldi is adapted to targeting the dominant poles within the given spectrum. The following criteria help to define the wanted eigenvalues.

(i) $f_s < Im(s_i) \leq f(e)$

(ii) $\rho(s_i)/\rho_{\max} > p$ with $\rho(s_i) = \frac{R_i}{Re(s_i)}$

The former places a limit to the imaginary part of the poles corresponding to the segment boundary. And the latter is used to estimate the dominance ρ defined by the ratio of the residue $R(s_i)$ to the real part $Re(s_i)$. The threshold of p serves to check the dominance of s_i in reference to the greatest ρ achieved so far. only the poles satisfying the both criteria are of our interest and ought to be identified by Q-arnoldi.

In order to accelerate the convergence towards the interior poles of a given spectrum, we apply a shift-and-invert Q-arnoldi via a spectral transformation $f(s) = 1/(s - s_0)$ where $s_0 = j2\pi f_0$ is at the center of

the spectrum. As a result, the sequence to be converged is in the inverse order of the distance to s_0. Specifically speakinh, the eigenvalues with imaginary part close to $2\pi f_0$ converges fast. In addition, because s_0 is located at the imaginary axis, convergence tends to the ones having small real part, one typical identity of a dominant pole. In a word, the proposed method favors the convergence towards the interior of the spectrum, especially the dominant ones.

Q-arnoldi will proceeds iteratively until fulfilling the expectation of the computation. However,the growing iterations will increase the dimension of the subspace and therefore increase the storage and computational cost. One remedy is to perform a restart, a process of reducing the subspace by throwing away that part that is unlikely to significantly contribute to the convergence of the wanted eigenvalues. In this paper, approximates failing to satisfy the above criteria are purged via implicit restarting [11], thus further accelerating the convergence towards the desired ones. Once all approximates are purged even after a plenty of explorations, it seems the time to close the Q-Arnoldi by reasoning that none of desired poles indeed exist within the specified spectrum. The other condition of terminating the process is that the convergence reluctantly happens to the undesired one, which implies that there has no extra poles deserving the further computation.

To sum up, with the Q-arnoldi method, the dominant poles and residues of Q_1 and Q_2 can be computed automatically and efficiently.

3.3. Compensation of the Poles out of Band

The truncation of the spectrum at the extremely high and low frequencies might miss the dominant poles over there. Generally, the effect can be simulated by a series of asymptotic terms [20] and the model can be completed by incorporating them

$$Q(s) = \sum \frac{R_i}{s - s_i} + \sum \frac{R_i^*}{s - s_i^*} + \frac{T}{s} + \left[E_0 + E_1 s + E_2 s^2\right] \qquad (19)$$

$\frac{T}{s}$ accounts for the contribution of poles below the bandwidth of interest while $[E_0 + E_1 s + E_2 s^2]$ compensates poles at the higher frequency. The points already computed for the derivation of $\mathbf{Z}(s)$ can be further used to estimate the coefficients via interpolating the deviation between the approximate model (18) and the exact solutions.

4. NUMERICAL RESULTS AND DISCUSSIONS

An example is given here to test the performance of the proposed method. The band under investigation spans from $f_L = 1$ GHz to

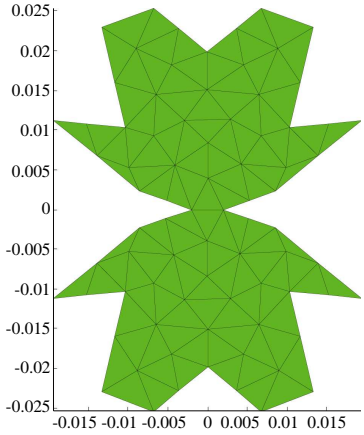

Figure 2. Mesh of antenna.

Table 1. Solution to segmentation.

No	1	2	3	4
Solution 1 (GHz)	$[1, 2]$	$[2, 4]$	$[4, 8]$	$[8, 12]$
Solution 2 (GHz)	$[1, 1.5]$	$[1.5, 3]$	$[3, 6]$	$[6, 12]$

$f_H = 12$ GHz. In order to test the generality of this method, we use an arbitrary antenna picked by a shape generator [21] (as shown in Fig. 2) as an illustration. Regardless of the specific configuration, only the maximum dimension $R_{\max}$ is of concern for confining $\triangle f_{\max}$. In this case $R_{\max} = 0.052$ m, $\triangle f_{\max}$ approximate 3 GHz. According to the recursion step introduced by (17), two solutions are presented in Table 1. Solution 1 carries segmentation from f_L, whereas Solution 2 performs reversely. However, both is consisted of 4 segments. If segments are connected end to end, only 9 points is needed for deriving $\mathbf{Z}(s)$. Based on the quadratic approximation of $\mathbf{Z}(s)$ within each segment, the input impedance is calculated and plotted in Fig. 3, which verifies that both solutions provide good agreement to the exact solution. The following results is based on Solution 1.

Subsequently, Q-Arnoldi is implemented. The initial dimension of subspace is chosen to be 10; convergence tolerance is set to 10^{-10}, and the dominance threshold p is specified to 10%. Table 2 lists the final results. Depended on these 4 poles s_i and residues R_i, reduced models of Q_1 and Q_2 can be established according to (18). The approximate results shown in Fig. 4 and Fig. 5 indicate the reduced models are capable of capturing the significant tendencies. Resonances happen at

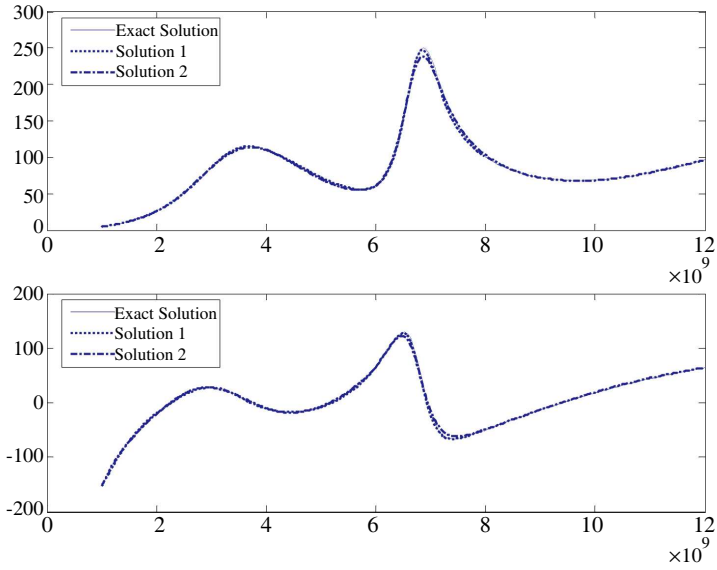

Figure 3. Approximate input impedance.

Table 2. Poles and residues.

s_i (GHz)	R_i of Q_1 ($\times 10_{-3}$)	R_i of Q_2 ($\times 10_{-3}$)
$-0.3400 + 2.0620j$	$-0.2672 - 0.1217j$	$0.8578 + 0.4409j$
$-0.5897 + 5.6621j$	$0.1886 + 0.0578j$	$0.5491 - 0.5936j$
$-1.5559 + 9.4470j$	$0.1078 + 0.3106j$	$1.7762 - 0.0446j$
$-2.8700 + 11.9520j$	$0.0024 + 0.0053j$	$0.6716 - 0.2228j$

the frequencies near the imaginary part of poles. As shown in both Fig. 4 and Fig. 5, Q_1 and Q_2 achieved local minimum or maximum around 2.0620 GHz and 5.6621 GHz. Though the intensity is not so severe as the former two, the resonant tendency can be also detected around 9.4470 GHz and 11.9520 GHz. The mismatch to the exact solution is attributed to the neglect of the dominant poles outside and is addressed through the compensation of (19). The refined models of (19) result in the improved accuracy and agreement with exact solutions, as also plotted Fig. 4 and Fig. 5.

Based on reduced models of Q_1 and Q_2, $H_{TA}(s)$ can be synthesized according to (9) and the result has been presented in Fig. 6, which validates the accuracy of our approach. It should be noted that the propagation term $\frac{e^{\frac{-sR}{c}}}{4\pi R}$ is left out of the result for a better resolution of comparison.

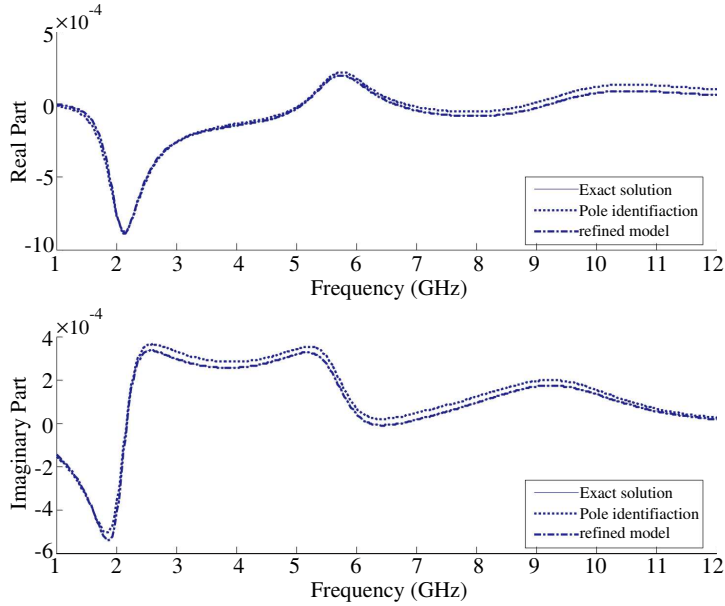

Figure 4. Model of Q_1.

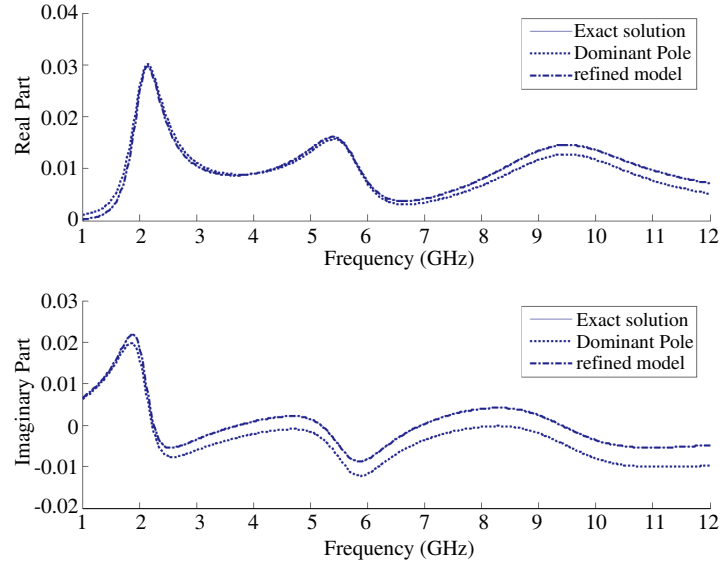

Figure 5. Model of Q_2.

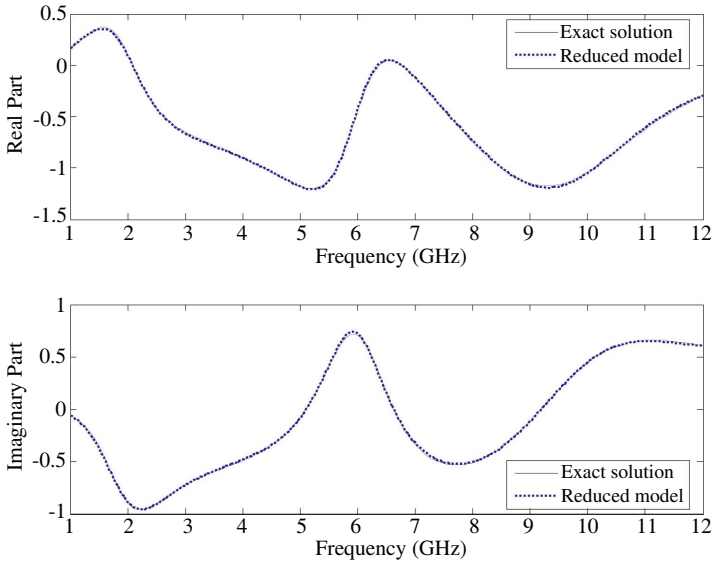

Figure 6. Model of $H_{TA}(s)$.

For this example, some features can be summarized as follows:

- Throughout this example, only 4 segments are involved and only 9 points are needed not only for the derivation of $\mathbf{Z}(s)$, but also for the estimation of the coefficients of asymptotic terms in (19). In addition, model-building only depends on 4 dominant poles with the fast identification of Q-Arnoldi. These facts strongly prove the substantial saving on the computational time.
- Throughout this example, no human factors are involved and no knowledge specific to the problem are needed except for the maximum dimension of the antenna body.

5. CONCLUSIONS

This paper has proposed a method capable of fulfilling a reduced model of transfer function of a UWB antenna system. The process is free of any human factor and suitable for any antenna system. The benefits of this method is several folded. The first is that the efficiency has been highly enhanced. In a sense, only the points required to interpolate $\mathbf{Z}(s)$ are directly computed and only the dominant poles are identified by handling a low dimensional model. Therefore, the computation cost has been substantially reduced. The second is that it largely reduces

the risk of yielding the nonphysical results such as the pseudo poles since the method is founded upon the physical formulations instead of purely depending on the samples. Another remarkable feature of this approach is that separate modeling of Q_1 and Q_2 allows for the separate analysis and design of the feeding model and the propagation channel. For example, the characteristics of Q_2 provide the practical guidelines for the design of the feeding model or the loading model such as the coplanar waveguide, which is widely adopted for broadening the bandwidth of UWB antennas. The characteristics of Q_1 are helpful to construct the appropriate propagation channel. Therefore, the separate analysis of Q_1 and Q_2 leads to more insightful understanding of the entire antenna system.

REFERENCES

1. Zwierzchowski, S. and P. Jazayeri, "A systems and network analysis approach to antenna design for UWB communications," *Journal Title Abbreviation*, Vol. 1, 826–829, 2003.
2. Chen, Z. N., X. H. Wu, H. F. Li, N. Yang, and M. Y. W. Chia, "Considerations for source pulses and antennas in UWB radio systems," *Journal Title Abbreviation*, Vol. 52, 1739–1748, 2004.
3. Qing, X. M., Z. N. Chen, and M. Y. W. Chia, "Network approach to UWB antenna transfer functions characterization," *The European Conference on Wireless Technology 2005*, 293–296, 2005.
4. Zhang, Z. and Y. H. Lee, "A modified model-based interpolation method to accelerate the characterization of UWB antenna system," *IEEE Trans. Antennas Propagat.*, Vol. 55, 475–479, 2007.
5. Rego, C. G. C., J. S. Nunes, and M. N. De Abreu Bueno, "Unified characterization of UWB antennas in time and frequency domains: An approach based on the singularity expansion method," *IMOC 2007*, 827–831, 2007.
6. Duroc, Y., R. Khouri, V. T. Beroulle, P. Vuong, and S. Tedjini, "Considerations on the characterization and the modelization of ultra-wideband antennas," *ICUWB 2007*, 491–496, 2007.
7. Licul, S. and W. A. Davis, "Unified frequency and time-domain antenna modeling and characterization," *IEEE Trans. Antennas Propagat.*, Vol. 53, 2882–2888, 2005.
8. Antoulas, A. C., *Approximation of Large-Scale Dynamical Systems*, Society for Industrial and Applied Mathematic, 2005.
9. Miller, E. K., "Model-based parameter estimation in electro-

magnetics. II. Applications to EM observables," *IEEE Antennas Propag. Mag.*, Vol. 40, 51–65, 1998.

10. Zhao, Z. Q., C.-H. Ahn, and L. Carin, "Nonuniform frequency sampling with active learning: Application to wide-band frequency-domain modeling and design," *IEEE Trans. Antennas Propagat.*, Vol. 53, 3049–3057, 2005.
11. Meerbergen, K., "The Quadratic Arnoldi method for the solution of the quadratic eigenvalue problem," *SIAM. J. Matrix Anal. Appl.*, Vol. 30, No. 4, 1463–1482, 2008.
12. Makarov, S. N., *Antenna and EM Modeling with Matlab*, Wiley-Interscience, 2002.
13. Rao, S., D. Wilton, and A. Glisson, "Electromagnetic scattering by surfaces of arbitrary shape," *IEEE Trans. Antennas Propagat.*, Vol. 30, 409–418, 1982.
14. Duroc, Y., V. Tan-Phu, and S. Tedjini, "A time/frequency model of ultrawideband antennas," *IEEE Trans. Antennas Propagat.*, Vol. 55, 2342–2350, 2007.
15. Virga, K. L. and Y. Rahmat-Samii, "Efficient wide-band evaluation of mobile communications antennas using $[Z]$ or $[Y]$ matrix interpolation with the method of moments," *IEEE Trans. Antennas Propagat.*, Vol. 47, 65–76, 1999.
16. Newman, E. H., "Generation of wide-band data from the method of moments by interpolating the impedance matrix [EM problems]," *IEEE Trans. Antennas Propagat.*, Vol. 36, 1820–1824, 1988.
17. Tisseur, F. and K. Meerbergen, "The quadratic eigenvalue problem," *SIAM Review*, Vol. 43, 235–286, 2001.
18. Bai, Z. J. and Y. F. Su, "SOAR: A second-order arnoldi method for the solution of the quadratic eigenvalue problem," *SIAM J. Matrix Anal. Appl.*, Vol. 26, 640–659, 2004.
19. Rommes, J. and N. Martins, "Efficient computation of transfer function dominant poles of large second-order dynamical systems," *SIAM J. Sci. Comput.*, Vol. 30, 2137–2157, 2008.
20. Balmés, E., "Model reduction for systems with frequency dependent damping properties," *International Modal Analysis Conference*, 1996.
21. Persson, P. O. and G. Strang, "A simple mesh generator in MATLAB," *SIAM Review*, Vol. 46, 329–345, 2004.